T.3: Studies on few important nuclear materials at the x-ray fluorescence microprobe and angle dispersive XRD beamlines on Indus-2

M. K. Tiwari[1] and A. K. Sinha
Hard X-ray Applications Laboratory
Synchrotrons Utilization Section
[1]*Email: mktiwari@rrcat.gov.in*

Abstract

In the recent past, experiments involving nuclear materials have been performed using x-ray fluorescence microprobe beamline (BL-16) and angle dispersive x-ray diffraction (ADXRD) beamline (BL-12), on Indian synchrotron source, Indus-2. High flux, photon energy tunability and low emittance of the synchrotron source have been utilized to answer critical questions involving different nuclear materials like uranium and thorium oxides, doped oxides, purity of reactor grade graphite, zircaloy etc. In this article, we shall discuss work done at these two beamlines related to departmental applications.

1. Introduction

Synchrotron radiation sources offer several orders of magnitude higher photon flux, lower emittance than the laboratory x-ray sources and tunable x-ray photon energies. These properties are extremely useful for cutting edge research, not possible using laboratory x-ray sources. Such a source becomes even more important for research related to nuclear and other strategic materials, because scientific data are not available in the public domain. In recent past, Indian synchrotron source, Indus-2, has been extensively utilized for the characterization of nuclear materials, resulting in answers to some critical questions related to the applicability of some of these materials, in nuclear reactors. In this article, we shall discuss characterization and other related applications of nuclear materials using x-ray fluorescence (XRF) and x-ray diffraction (XRD) techniques on XRF microprobe beamline (BL-16) and angle dispersive XRD (ADXRD) beamline (BL-12), respectively. X-ray fluorescence spectroscopy is an important non-destructive method for the elemental analysis of materials at the micro and trace levels. It finds variety of applications in different fields (viz. geology, archaeology, biomedical science and material science, nuclear industry etc.) [1,2]. XRD technique, on the other hand, studies the crystal structure of crystalline and poly-crystalline materials and can comment on suitability of a material for given application. Extreme conditions XRD measurements predict the behavior of a material at actual working conditions of high pressures and high temperatures. The XRF beamline (BL-16) has been installed on a bending-magnet source and works in the x-ray energy range 4–20 keV. The beamline is equipped with Si(111) based double crystal monochromator (DCM) and Kirkpatrick–Baez (KB) mirror focusing system. The beamline provides both micro-focused and collimated x-ray beam modes at the experimental station. Using the micro focused mode of the BL-16 beamline, it is possible to examine a sample for spatial distribution of elements. The beamline also allows a user to perform ultra-trace elemental analysis using its total reflection x-ray fluorescence (TXRF) operational mode. The details of the BL-16 beamline are given elsewhere [3]. ADXRD beamline (BL-12) has also been installed on a bending magnet and comprises of a Si(111) based DCM with sagittally bendable second crystal optics to focus x-ray beam in the sagittal plane. The x-ray focusing in the meridional plane is achieved using a cylindrical mirror. The beamline works in the x-ray energy range of 5-25 keV. The experimental stations of the beamline consist of a 6-circle diffractometer station with scintillation detector and an image plate area detector, which is especially suitable for the powder diffraction experiments. More details of the beamline have been described elsewhere [4]. In the following sections, we shall briefly describe different studies that have been carried out using the two beamlines on nuclear materials and outline the important conclusions drawn from these studies.

2. Mixed uranium–thorium oxides fuel

India has one of the largest reserves of thorium that can be utilized for electricity generation using different types of nuclear reactors [5]. Thorium-based fuel has certain advantages over uranium and plutonium fuels [6]. It has been proposed to use mixed thorium and uranium oxide based fuels [7]. To obtain better uniformity for the mixed uranium–thorium oxide fuel, comprising of low concentration (wt. %) of uranium, the fuel pellet is normally prepared by diluting uranium–thorium oxide mixtures containing higher uranium % with ThO_2. Estimation of uniformity of these pellets is very critical, which can be ensured using energy dispersive x-ray fluorescence (EDXRF) technique and micron size x-ray beam at BL-16. With this motivation, a study for the determination of uranium and thorium concentrations in mixed uranium–thorium oxide pellets was carried out and the quantification procedures were applied to estimate the spatial variation of U and Th in mixed oxide fuel pellets. Two critical questions were: (1) Which impurity phases exist in the pellets and their concentrations? (2) What is the spatial uniformity of U and Th elements in these fuel pellets?

2.1 Impurity phases

EDXRF measurements on uranium–thorium oxide pellets [8] containing ~ 45.3% uranium, with yttrium (Y) as an internal standard (amount ~ 47.1 mg), were carried out using laboratory source as well as synchrotron radiation source. The EDXRF spectrum measured using the synchrotron shows

higher detection sensitivity compared to that of laboratory source, although the time used for XRF measurement at laboratory source was ~ 300 s as compared to 100 s used for synchrotron measurements. This indicates that synchrotron source certainly provides better detection limit compared to a laboratory source.

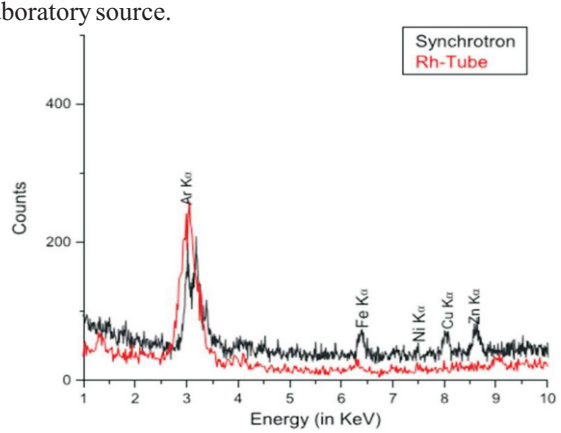

Fig. T.3.1: Comparison of expanded low energy region EDXRF spectra of representative of uranium–thorium oxide sample mixed with yttrium internal standard measured at laboratory and synchrotron sources.

From Figure T.3.1, it can also be seen that some of the impurity elements, *e.g.* Fe, Ni, Cu, and Zn that were not clearly visible in EDXRF spectrum measured using laboratory source, can be fairly distinguished in the synchrotron based XRF measurements. From the technical point of view, it is very important to quantify the presence of these trace elements in a fuel that may produce long lived radioisotopes. The measurements show the presence of Fe, Ni, Co, and Zn at ppb levels in the mixed uranium–thorium oxide fuel samples.

2.2 μ-XRF studies on compositional uniformity of uranium–thorium oxides fuels

Non-uniformity of U and Th in the fuel pellets is a critical issue. If the compositional non-uniformity in the fuel pellets is large, it will generate localized hot spots in a fuel pellet, during reactor operation at locations where the fissile material content is larger. This thermal gradient in the fuel pellets is non-desirable from the safety point of view. Various standard procedures are employed for the generation of uranium-thorium oxide fuel pellets. The conventional route employed for the production of such oxides fuel involves powder metallurgical compaction (PMC), comprising of blending of ThO_2 and UO_2 powders followed by milling, compaction, and sintering in reduced atmospheric environment at ~1700 °C. [9]. The PMC process however, produces high γ-radiation dose [5] in the range of 0.7– 2.6 MeV energies. Coated agglomerate pelletization (CAP) is another method suggested for the fabrication of such fuels. In CAP method, free flowing agglomerates of ThO_2 are prepared in the alpha active glove box. Subsequently, these particles are coated with ^{233}U oxide and compacted. The details of the CAP process are given elsewhere [10]. Although, CAP avoids radiation exposure to the personnel up to a certain level, the pellets produced by this method are prone to drawback of non-uniformity because of the non-homogeneous mixing procedure adopted.

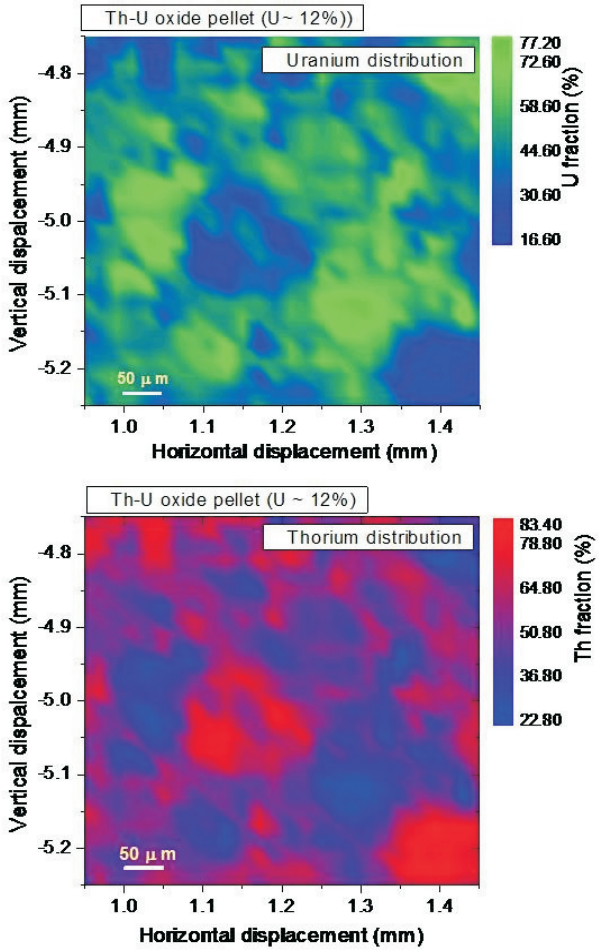

Fig. T.3.2: Measured distribution of uranium and thorium obtained from μ-XRF study on a ThO_2 – 12% UO_2 pellet prepared by CAP route.

In order to assess the compositional uniformity of the PMC and CAP route-prepared uranium–thorium oxides fuel pellets microprobe x-ray fluorescence mapping of the different elements have been carried out using BL-16 beamline. Distribution of U-Lα and Th-Lα intensities (representing uranium and thorium concentrations) in the CAP route pellet having ~ 12% uranium is shown in Figure T.3.2. Similar distribution of uranium and thorium in PMC route-prepared

ThO_2 – 12% UO_2 pellet is shown in Figure T.3.3. It can be seen that both thorium and uranium distributions in the CAP route-prepared pellets have larger non-uniformity compared with similar pellets prepared using the PMC route. The non-uniformity in CAP route-prepared pellets is due to the variation in relative amounts of uranium and thorium at different spots.

Although synchrotron sources are not suited for such routine applications, the present study has given a direction for chemical quality assurance of nuclear fuel for its uniformity. More details about x-ray fluorescence mapping of uranium–thorium oxides fuel pellets are given elsewhere [11].

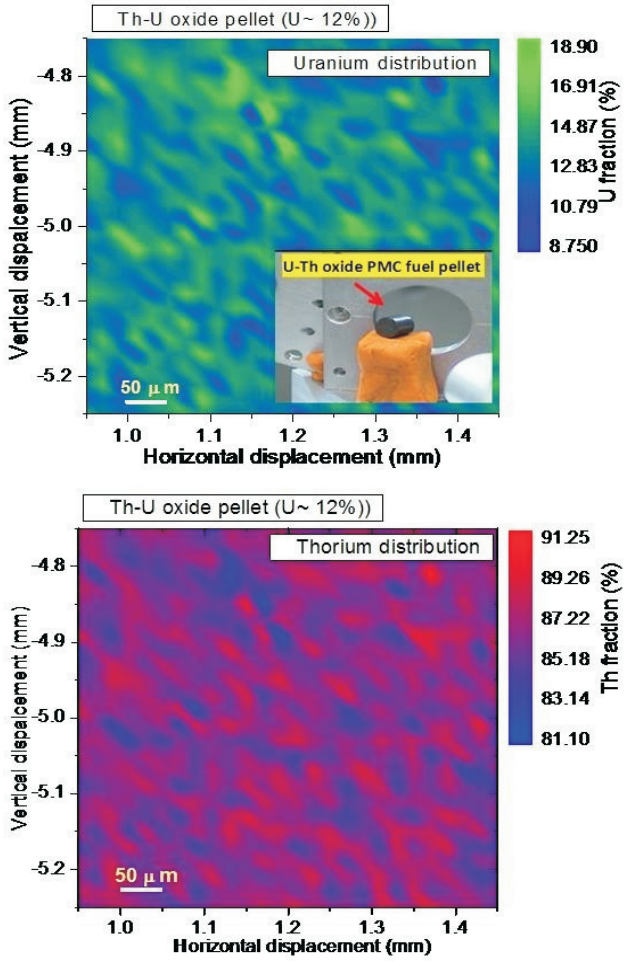

Fig. T.3.3: Measured distribution of uranium and thorium obtained from µ-XRF study on a ThO_2 – 12% UO_2 pellet prepared by PMC route. In the inset of top panel, actual mounting of PMC fuel pellet is shown.

3. Determination of oxidation states of nuclear fuel materials

Oxides of uranium are important nuclear materials. These oxides in different oxidation states crystallize in different structures, resulting in compounds with drastically different mechanical, thermal and electrical properties. UO_2 generally crystallizes in a fluorite structure [12]. But in a varied oxidation conditions, it may get converted into other oxides, such as U_4O_9, U_3O_7, U_3O_8 etc. [13]. Precise knowledge of the oxidation states of uranium in these oxides as well as in other compounds of uranium is extremely important to understand the properties of these compounds, and use them efficiently for different applications. Apart from this, such studies are also very helpful in understanding their behavior during real operating conditions of a reactor as well as during spent fuel reprocessing [14]. U_3O_8 is a stable oxide of uranium and exists primarily in three different phases. At room temperature its phase comprises orthorhombic structure. However, at high temperatures it is composed of two other phases having hexagonal and tetragonal lattice structures [15]. U_3O_7 is another oxide of uranium which exists in the metastable state. The mixed-valent oxidation state of uranium in U_3O_8 can be represented in two ways by preserving the charge balance neutrality, as shown below:

$$U_3O_8 = U^{VI}U_2^{V}O_8 \text{ or } = U_2^{VI}U^{IV}O_8$$

Similarly, for U_3O_7, there are two probable combinations of oxidation states:

$$U_3O_7 = U_2^{IV}U^{VI}O_7 \text{ or } = U_2^{V}U^{IV}O_7$$

X-ray absorption near edge spectroscopy (XANES) is an established technique to estimate average oxidation state of an element in the sample. It is known that the photon energy of absorption edge of an element blue shifts with the increase in its oxidation state. The shift in absorption edge energy scales linearly with the change in oxidation state. This property is exploited in estimating average oxidation state of an element in the sample by measuring XANES spectra of the unknown sample along with the spectra for some standard samples. However, a normal XANES measurement in either absorption or reflection mode needs a large quantity of sample, an undesirable option when working with radioactive materials. We have proposed total reflection x-ray fluorescence (TXRF) based XANES measurement which needs only a tiny amount of sample. TXRF is a variant of the EDXRF technique. It finds wide applications in different scientific and technological areas [16]. The potential advantage of TXRF technique is that it requires very small amount of a sample specimen. It is highly suitable for the study of nuclear materials as it offers advantages of comparatively lower radiation hazard to the operator as well

as generates a very small amount of radioactive waste. Because of all these features TXRF assisted XANES measurements have been carried out at the BL-16 beamline. Only a tiny amount (a few nano grams) of the uranium oxides specimens were taken directly on the quartz glass sample supports with the help of a micro-pipette tip. These particles were then spread uniformly on top of the TXRF sample supports. More details of TXRF experimental station on BL-16 beamline, that was utilized for the TXRF assisted XANES measurements of uranium oxide fuel samples may be found in [17]. The absorption coefficient is then estimated from the intensity of U-L_α line as shown in Figure T.3.4, which shows a typical TXRF spectrum for uranium oxide (U_3O_8) sample. The absorption coefficients, thus obtained for different U compounds, at energies between 17.18 and 17.28 keV are plotted in Figure T.3.5.

From the recorded TXRF spectrum for U_3O_8 sample (Figure T.3.4), it can be seen that only a few nano grams amount of specimen is sufficient to provide reasonable magnitude of x-ray intensities of U-L and U-M lines, for an acquisition time of 10 s. The spectrum was recorded using incident excitation x-ray energy of E_0~ 17.16 keV. Earlier, it was already shown that the particle size of the analytes that stick on the TXRF sample support when one follows a single rubbing process of a fuel pellet ranges between 200 and 500 nm [16].

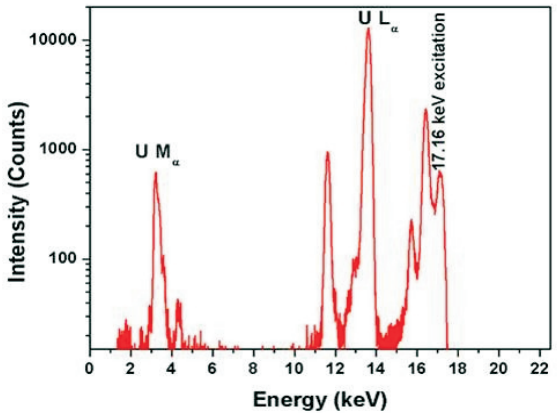

Fig. T.3.4: Recorded TXRF spectrum of U_3O_8 specimen.

In the present study [17], similar sample preparation method was adopted while carrying out TXRF assisted XANES measurements of mixed U-Th oxide fuel pellets. Figure T.3.5 shows the measured normalized TXRF-XANES spectra of different uranium oxide compounds UO_2, $TlUO_3$, U_3O_8, and UO_3 respectively. From this figure, it can be seen that, as the oxidation state of uranium increases from 4 to 6 (for UO_2 to UO_3), the position of the U-L_3 edges in the XANES spectra are shifting toward the higher energy side in an obvious manner.

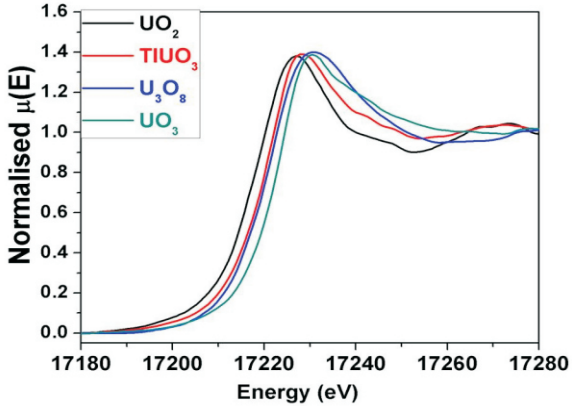

Fig. T.3.5: Measured TXRF-XANES spectra of U_3O_8 along with different standard compounds.

The exact edge energy positions were obtained from the maxima of first derivative of the recorded XANES spectrum.

The percentages of different oxidation states of U present in U_3O_8 fuel was determined using linear combination analysis of the XANES spectra with ATHENA software. During spectra fitting, two combinations of oxidation states of U were considered. (1) U(IV) and U(VI), and, (2) U(V) and U(VI).

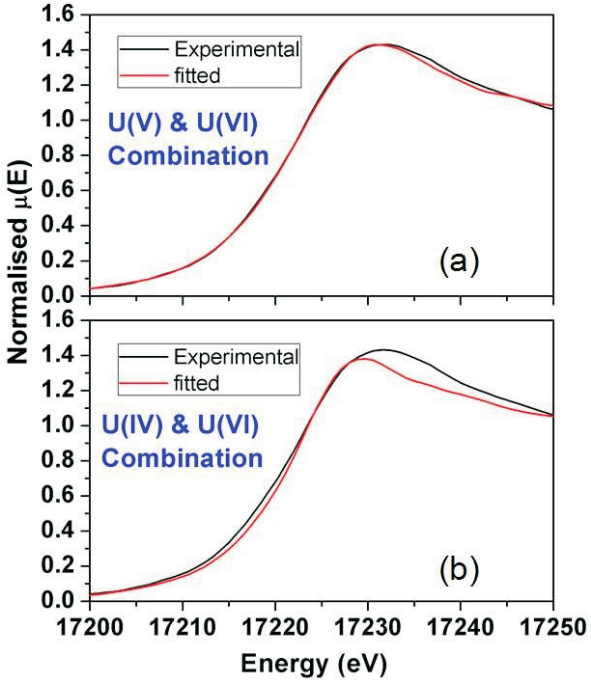

Fig. T.3.6: Linear combination fitting of TXRF-XANES spectra of U_3O_8 using combinations of two different oxidation states; (a): U (V) + U (VI), and, (b): U (IV) + U (VI), respectively.

The best fitted results for the two cases (top and bottom panels), respectively are demonstrated in Figure T.3.6. These results provided percentage values of different oxidation states U(V) ~ 70%, U(VI) ~ 30% present in the U_3O_8 fuel (as compared to that of the expected values of 66% and 34%, respectively). Similarly, in the case of U_3O_7, the uranium was found to be in mixed-valent states of U(IV) and U(VI) having percentage fractions of ~ 70% and 30%, respectively. These values were found to be in agreement with the theoretically calculated values. The technique offers potential advantages in the case of the chemical state analysis of radioactive nuclear materials as it requires sample amount in nanogram levels only, with no rigorous sample preparation requirements.

4. Trace elements in high purity graphite moderators

High purity graphite is utilized as moderator as well as reflector in nuclear reactors. It is also used as precursor for nuclear fuels in the fast breeder test reactor. Precise knowledge of the presence of different trace elements and their contents in graphite is essential for evaluating its quality control for the above described applications. In the synchrotron radiation based x-ray florescence measurements, the advantage of incident x-ray energy tunability offers high detection sensitivities for various trace elements (at ultra-low quantity) present in the graphite matrix. Such measurements are especially important to identify those trace elements that generate long lived isotopes in the nuclear waste. Using the BL-16 beamline of Indus-2 facility two different incident x-ray energies 12 keV and 20 keV respectively, were used to determine of Ca, Cr, Mn, Fe, Ni and Zn, and Sr, Zr and Pb elements in high purity graphite specimens (Figure T.3.7). Quantification of these elements were carried out using Ga internal standard of amount ~ 10 ppm.

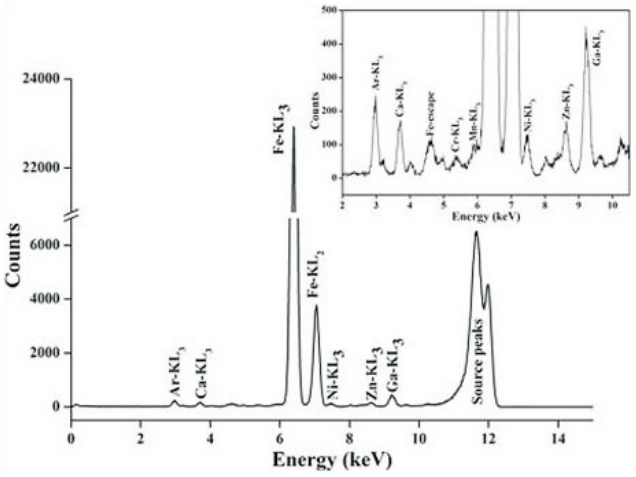

Fig. T.3.7: Measured SRXRF spectrum of a graphite sample with Ga internal standard (10 ppm) at E_0 ~ 12 keV.

It was realized that SRXRF could improve the detection limits of Ca, Cr, Mn, Fe, Ni, Zn, Sr, Zr and Pb in graphite by an order of magnitude with respect to the laboratory based EDXRF measurements. More details have been described elsewhere [18].

5. Determination of M sub shell x-ray emission cross sections of some of the nuclear materials

The probability of photon induced fluorescent x-ray emission that is usually termed as x-ray production cross section or x-ray fluorescence cross section (σ^*) is an important parameter. This quantity finds potential applications in various fields such as radiation shielding, material science, atomic and molecular physics, forensic science, dosimetric computation, and industrial irradiation processes. This composite parameter is defined as the product of photo ionization cross section, fluorescence yield and fractional radiative decay rates [19]. For the medium atomic number elements ($67 \leq Z \leq 92$) measured experimental data for L x-ray fluorescence cross sections are available in literature [20], but data on M x-ray production cross section is rather scanty because of its structural complexities. M shell consists of five sub-shells and it is difficult to have selective excitation of an individual sub-shell due to relatively small energy differences among different sub-shells. While measuring the x-ray production cross-section of an element, considerations about the incident photon source is important because the x-ray emission probability strongly depends on the incident photon energy. A synchrotron radiation based beamline provides very high incident photon flux and also selective incident energies for the excitation of a material. BL-16 beamline of Indus-2 facility has been utilized to determine M-sub shell x-ray emission cross sections of different elements Pt, Au, Hg, Pb,

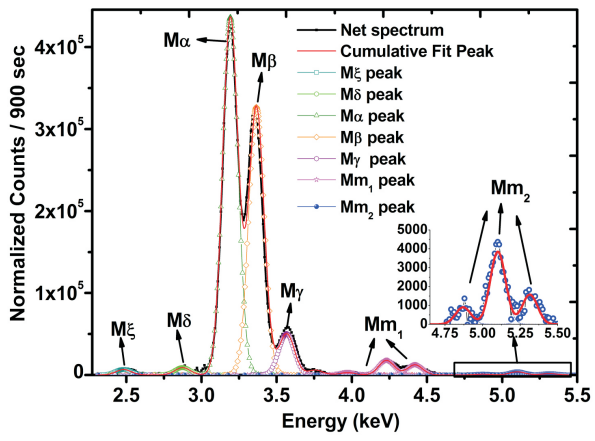

Fig. T.3.8: Unfolding of different M x-ray fluorescence lines (M_ξ, M_δ, M_α, M_β, M_γ, M_{m1} and M_{m2}) for uranium M x-ray fluorescence spectrum measured at 8 keV x-ray energy.

Th and U at x-ray photon energy of 8 and 10 keV. Figure T.3.8 shows the background subtracted spectrum of U. The details about measured and theoretical values of M x-ray production cross sections of uranium and thorium are given elsewhere [19].

6. Depth resolved elemental analysis of zircaloy using grazing incidence XRF (GIXRF) technique

Zirconium alloys find wide spread applications in the nuclear industry. A variety of zirconium based alloys are used because of their physical strength, chemical corrosion resistance and thermal properties for cladding materials and pressure tubes

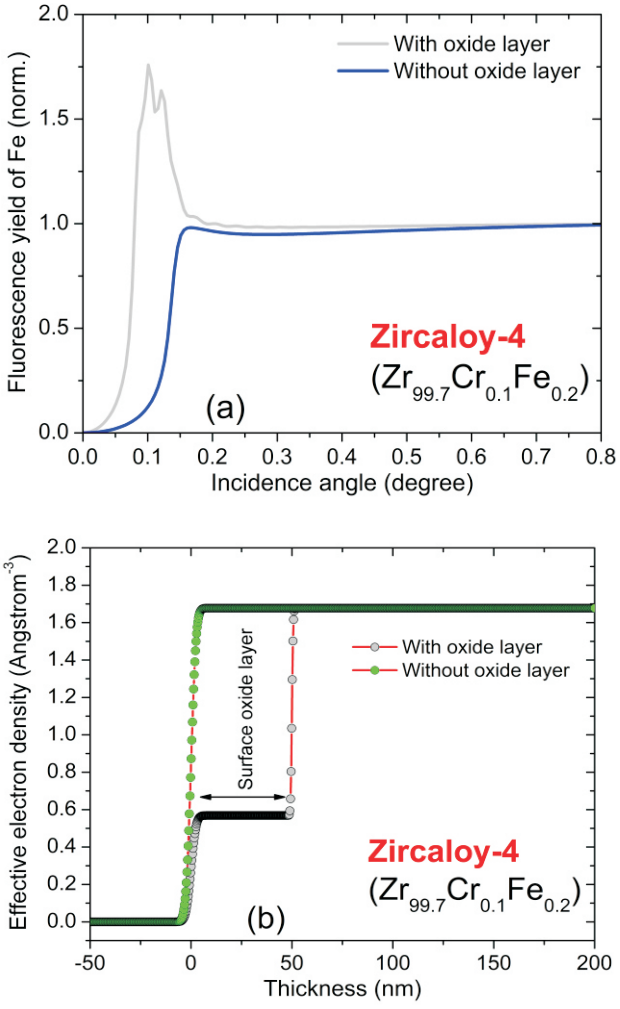

Fig. T.3.9: (a) shows computed angle dependent GIXRF of Fe-Kα intensity emitted from a polished Zircaloy-4 alloy in the two conditions of a low density surface oxide layer, (b) depicts effective electron density profiles in the two conditions.

in nuclear reactors [21]. Zircaloy materials have very low capture cross section for the thermal neutrons. Zircaloy-2 (Zr-Sn-Fe-Ni-Cr alloy) and Zircaloy-4 (Zr-Sn-Fe-Cr alloy) are widely utilized as cladding materials. The addition of Nb increases the mechanical strength of the material [22]. From corrosion point of view, the zirconium alloys as cladding material, encounter two types of corrosion mechanisms; one arising due to the interactions between cladding material and the coolant water on the outer surface. The second process involves interaction of cladding material with the fuel material and fission products produced inside the tube. Under the extreme conditions of temperature and environment in a nuclear reactor, the corrosion of zirconium alloys by coolant water/steam results in the growth of uniform oxide films on the cladding surface (outer surface of the tube). Stringent guidelines and specifications have been defined for the amount of trace elements present in these alloys and they need to be strictly monitored and retained during the fabrication of these alloys for the safe and efficient operation of the reactors.

These specifications are usually set by the reactor physicists on the basis of the type of the reactor. One of the utmost requirements is related to the concentration homogeneity of different trace elements present in these materials. Surface precipitations, oxide layer formation, in-depth inhomogeneity of different elements are major concerns that define their susceptibility to corrosion. Here, we have applied grazing incidence x-ray fluorescence (GIXRF) technique to study depth resolved concentration distribution profiles of different elements present in these materials. The details of this technique are described elsewhere [23]. Figure T.3.9(a) shows computed GIXRF of Fe-K_α intensity originated from a polished Zircaloy-4 alloy without considering any top surface

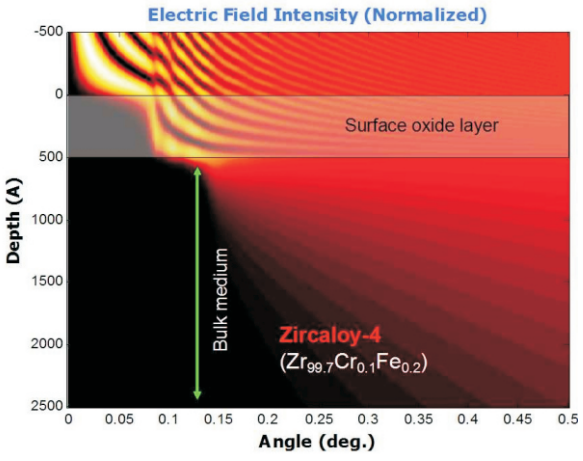

Fig. T.3.10: Computed x-ray intensity distribution profile inside Zircaloy-4 alloy as a function of incidence angle of the synchrotron x-ray beam.

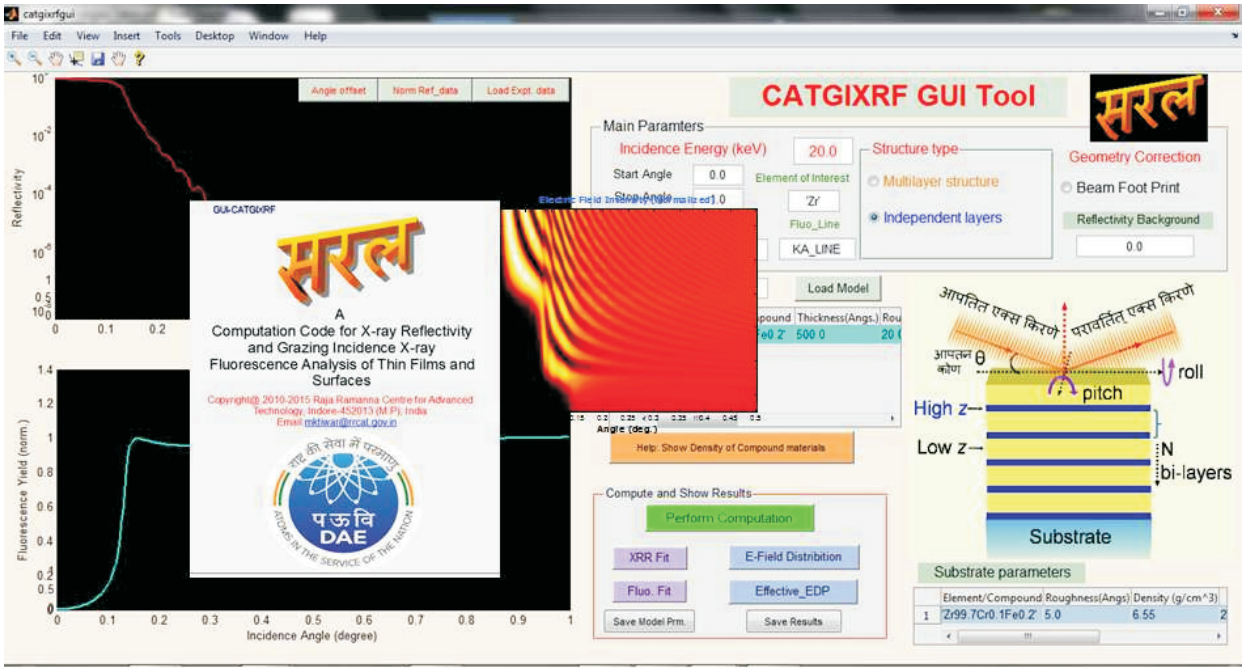

Fig. T.3.11: A snapshot of the GIXRF computation program developed at RRCAT, Indore [23].

oxide layer as well as in the condition of presence of a low density (~ 33 % of bulk density) surface oxide layer of thickness ~ 50 nm on top of it. Figure T.3.9(b) depicts computed effective electron density profiles in the two respective conditions.

From these figures, it can be clearly seen that GIXRF profile of an element is fairly sensitive to the change of density of the material as well as its in-depth location inside zirconium alloy. Figure T.3.10 demonstrates computed x-ray intensity distribution profile inside Zircaloy-4 alloy in the condition when a low density surface oxide layer is considered on top of it. Figure T.3.11 provides a snapshot of the GIXRF computation program developed at RRCAT, Indore for in-depth analysis of a material in non-destructive manner.

7. Structural characterization

Structural phase changes may cause major changes in thermal expansion and bulk modulus of material, leading to cracks or swelling etc. Real operating conditions of nuclear reactors are hostile, having high pressure, high temperature in addition to high radiation. Even when no phase transformation occurs, anomalous behavior of thermal expansion and bulk modulus have been observed under extreme conditions of temperature, pressure and radiation. Hence, prior crystalline structural knowledge for the materials in the reactors including under extreme conditions is mandatory. In the following, we discuss structural investigations on some important reactor material using ADXRD beamline (BL-12) on Indus-2.

7.1 High pressure XRD studies on UZr_2

U-Pu-Zr alloy is a possible fuel material for metallic fuel based fast reactor. A typical fuel contains about 23% Zr. Due to the thermal gradient generated in the fuel pin during operation, redistribution of Zr and U takes place making the central part of the fuel pin Zr rich. At higher burn up of fuel γ

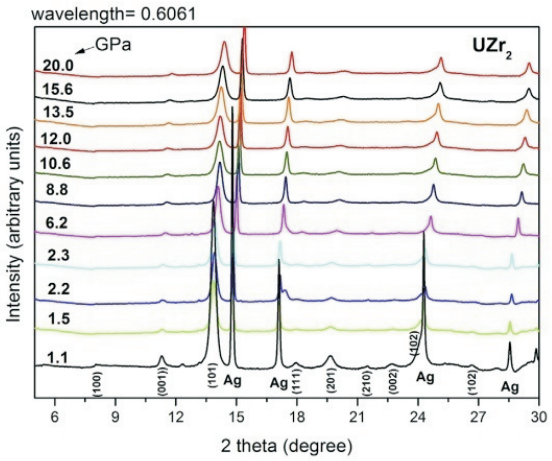

Fig. T.3.12: Measured XRD pattern of UZr_2 as a function of pressure (~ 0.6061 Å).

and δ phases of UZr_2 may form. Hence, it is required to study the high pressure and high temperature phase changes in this alloy. Using ADXRD beamline, we have studied high pressure XRD of the alloy up to 20 GPa, in order to address the following questions: (a) Is there any crystalline phase change in the given pressure range? (b) What are the bulk modulus and the pressure derivatives, in this pressure range? Figure T.3.12 shows the XRD pattern of UZr_2 as a function of pressure. These patterns have been analyzed using Rietveld refinement. A typical refined pattern is depicted in Figure T.3.13.

Lattice parameters and unit cell volume are obtained from the Rietveld analysis and bulk modulus as well as the pressure derivative of the bulk modulus are estimated. We find the bulk modulus and the pressure derivative for UZr_2 are 108 GPa and 5.0 respectively at ambient temperature. The room pressure phase of modified CB32, AlB2 type structure (also called the δ structure) is intact till at highest probed pressure of 20 GPa. More details are described elsewhere [24].

7.2 Crystal structure of Bi_2UO_6

Uranates of different elements have been reported in literature extensively because these compounds are formed by reaction involving uranium in fuel with either a fission product or with cladding/coolant material, during reactor operation.

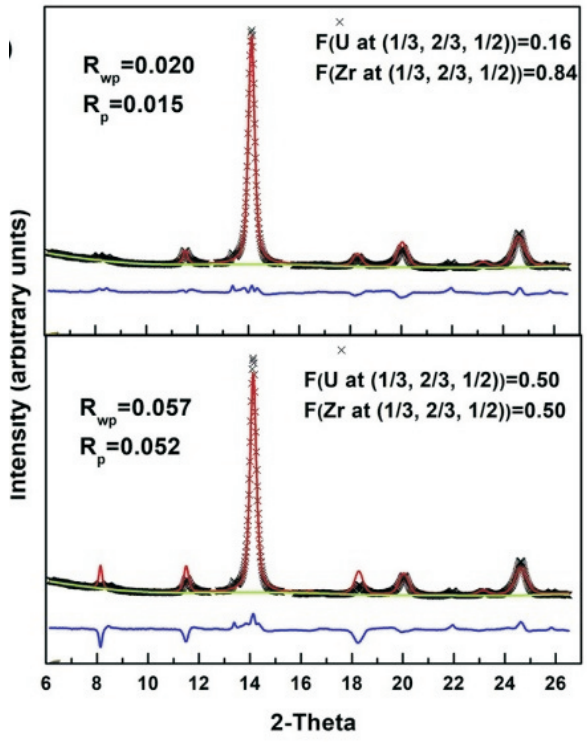

Fig. T.3.13: A typical refined pattern of UZr_2 alloy.

The densities of uranates are quite different compared to uranium oxides. Hence formation of uranates may result in the rupture of cladding material or swelling of fuel. Further doping of uranates of some other fission product is also possible. It may be mentioned that doping may change the properties of original compound drastically, raising some safety issues. Hence prior knowledge of crystalline structure of possible doped uranates is desirable. Formation of Sb doped Bi_2UO_6 is a possibility and no information is available in literature regarding this material. We, therefore, have studied the crystal structure of the system [25] using ADXRD beamline (BL-12). Figure T.3.14(a) shows the Rietveld refined XRD pattern for the system $Bi_{2-x}Sb_xUO_6$ for x = 0. In Figure T.3.14(b), we have shown expanded view of the XRD spectra for $Bi_{2-x}Sb_xUO_6$ (x = 0.04, 0.08, 0.12, 0.16).

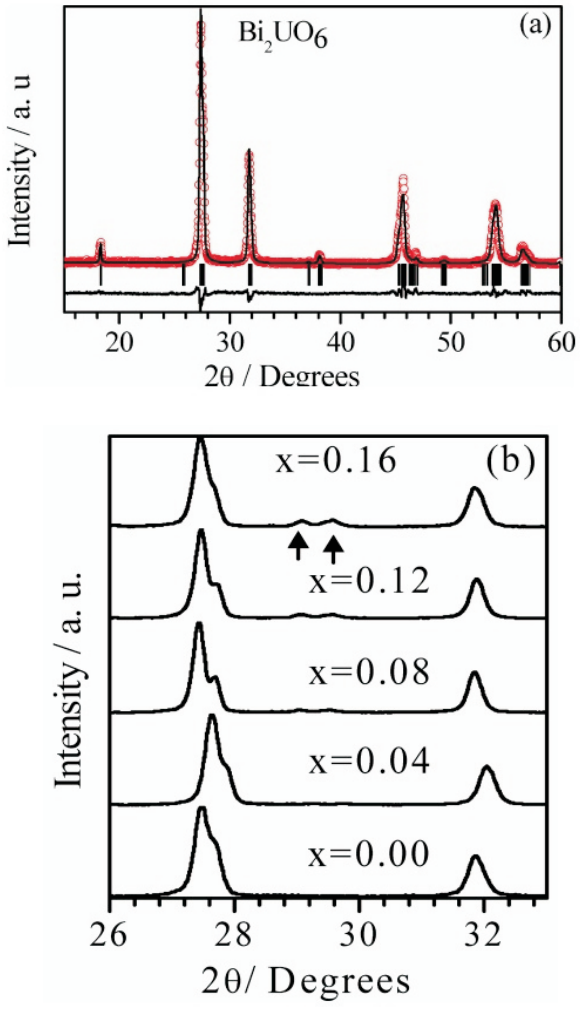

Fig. T.3.14: (a) Measured XRD pattern of pure Bi_2UO_6 sample, (b) shows an expanded XRD spectra for different Sb (x) doped Bi_2UO_6 samples.

A new Bragg peak starts to appear for higher Sb doping, probably because of the formation of a new phase. The unit cell parameters are found to decrease with the increase in doping and a new phase precipitates out for x > 0.06.

8. Summary and conclusions

Characterization of nuclear and other strategic materials in Indian facilities becomes more important because these are important national mandates. Towards this goal, important material aspects like crystal structure, trace impurities, elemental uniformity in a fuel pellets, x-ray interaction cross sections and depth resolved concentration analysis in important nuclear materials like U/Th oxides, high purity graphite, uranates, zirconium alloys, etc. have been studied using the microprobe XRF beamline (BL-16) and ADXRD beamline (BL-12) on Indus-2 synchrotron source. The following important conclusions have been drawn:

(i) PMC routed U/TH oxide pellets are more uniform than CAP routed pellets and these fuel pellets contain trace impurities of Fe, Co, Ni and Zn elements in ppb levels.

(ii) Mixed oxidation state of uranium oxide (U_3O_8) contains a mixture of U(V) and U(VI) oxidation states, whereas U_3O_7 contain a mixture of U(IV) and U(VI) oxidation states.

(iii) GIXRF technique can be employed for in-depth analysis of different elements present in zirconium and other alloy materials.

(iv) High pressure XRD studies show no phase transformation in UZr_2 up to 20 GPa.

Acknowledgments

The authors gratefully acknowledge support and encouragement from Dr. Tapas Ganguli, Head, SUS, Shri S. V. Nakhe, Director, LG and MSG and Shri D. Das, Director, RRCAT, Indore. Acknowledgments are also due to Dr. A. Sagdeo, Shri A. Upadhyay, Shri A. Bhisikar, Mrs. A. Trivedi, Shri M. N. Singh, Shri A. K. Singh and Shri A. Khooha for help in the work reported in this article. Contributions of the users, whose work has been included in the newsletter, are gratefully acknowledged.

References

[1] R. Klockenkamper, A. Von Bohlen, "Elemental analysis of environmental samples by total reflection x-ray fluorescence: a review", X-ray Spectrom., vol. 25, pp. 156–162, 1996.

[2] P. Pianetta, K. Baur, A. Singh, S. Brennan, J. Kerner, D. Werho, J. Wang, "Application of synchrotron radiation to TXRF analysis of metal contamination on silicon wafer surfaces", Thin Solid Films, vol. 373 pp. 222–226, 2000.

[3] M. K. Tiwari, P. Gupta, A. K. Sinha, S. R. Kane, A. K. Singh, S. R. Garg, C. K. Garg, G. S. Lodha and S. K. Deb, "A microfocus x-ray fluorescence beamline at Indus-2 synchrotron radiation facility", J. Synchrotron Rad. vol. 20, pp. 386–389, 2013.

[4] A. K. Sinha, Archna Sagdeo, Pooja Gupta, Anuj Upadhyay, Ashok Kumar, M. N. Singh, R. K. Gupta, S. R. Kane, A. Verma, and S. K. Deb, "Angle Dispersive x-ray Diffraction Beamline on Indus-2 Synchrotron Radiation Source: Commissioning and First Results", Journal of Physics: Conference Series, vol. 425, pp. 072017-18, 2013. doi:10.1088/1742-6596/425/7/072017.

[5] J. Banerjee, T. R. G. Kutty, A. Kumar, H. S. Kamath, S. Banerjee, "Densificstion Behaviour and Sintering kinetics of ThO_2-4% UO_2 pellet" J. Nucl. Mater., vol. 408, pp. 224-230, 2011.

[6] T. R. G. Kutty, M. R. Nair, P. Sengupta, U. Basak, A. Kumar, H. S. Kamath, "Characterization of (Th,U)O_2 fuel Pellets Made by Impregnation Technique" J. Nucl. Mater, vol. 374, pp. 9-19, 2008.

[7] R. K. Sinha, "Advanced Nuclear Reactor System: An Indian Perspective" Energy Procedia., vol. 7, pp. 34-50, 2011.

[8] N. L. Misra, M. K. Tiwari, S. Sanjay Kumar, Sangita Dhara, Ajit Kumar Singh, G. S. Lodha, S. K. Deb, P. D. Gupta and S. K. Aggarwal, "Synchrotron-induced EDXRF determination of uranium and thorium in mixed uranium–thorium oxide pellets", x-Ray Spectrom., vol. 42, pp. 4–7, 2013.

[9] T. R. G. Kutty, K. B. Khan, P. V. Achuthan, P. S. Dhami, A. Dakshinamoorthy, P. S. Somayajulu, J. P. Panakkal, A. Kumar, H. S. Kamath, "Characterization of ThO2–UO2 pellets made by co-precipitation process" J. Nucl. Mater., vol. 389, pp. 351-358, 2009.

[10] T. R. G. Kutty, K. B. Khan, P. S. Somayajulu, A. K. Sengupta, J. P. Panakkal, A. Kumar, H. S. Kamath, "Development of CAP Process of Fabrication of ThO2-UO2 fuels: Part I: Fabrication and Densification Behaviour" J. Nucl. Mater., vol. 373, pp. 299-308, 2008.

[11] N. L. Misra, M. K. Tiwari, Bal Govind Vats, S. Sanjay Kumar, Ajit Kumar Singh, G. S. Lodha, S. K. Deb, P. D. Gupta and S. K. Aggarwal, "Synchrotron μ-XRF study on compositional uniformity of uranium–thorium oxide pellets prepared by different processes", X-Ray Spectrom., vol. 43, pp. 152-156, 2014.

[12] L. Van Brutzel, A. Chartier, J. P. Crocombette, Phys. Rev. B, vol. 78, pp. 024111-7, 2008.

[13] F.J Grønvold, "High-temperature x-ray study of Uranium Oxides in the UO_2-U_3O_8 region" Inorg. Nucl. Chem., vol. 1, pp. 357- 370, 1955.

[14] D. R. Olander, "Fundamental Aspects of Nuclear Reactor Fuel Elements; Technical Report", TID-26711-P1, TRN: 08-019392; University of California: Berkeley, CA, 1- 629, 1975. doi: 10.2172/ 7343826 and *references therein*.

[15] Dickens, P. G., Powell, A. V.J., Solid State Chem., vol. 92, pp. 159- 169, 1991.

[16] N. L. Misra,, M. Singh Mudher, "Total Reflection x-ray Fluorescence: A Technique for Trace Element Analysis in Materials" Prog. Cryst. Growth Charact. Mater., vol. 45, pp. 65- 74, 2002.

[17] Kaushik Sanyal, Ajay Khooha, Gangadhar Das, M. K. Tiwari and N. L. Misra, "Direct Determination of Oxidation States of Uranium in Mixed-Valent Uranium Oxides Using Total Reflection x-ray Fluorescence x-ray Absorption Near-Edge Spectroscopy", Anal. Chem., vol. 89, pp. 871–876, 2017.

[18] M. Ghosh, K.K. Swain, P.S. Remya Devi, T.A. Chavan, A.K. Singh, M.K. Tiwari and R. Verma, "Determination of impurities in graphite using synchrotron radiation based x-ray fluorescence spectrometry", Applied Radiation and Isotopes, vol. 128, pp. 210–215, 2017.

[19] Gurpreet Kaur, Sheenu Gupta, M.K. Tiwari, Raj Mittal, "M sub shell x-ray emission cross section measurements for Pt, Au, Hg, Pb, Th and U at 8 and 10 keV synchrotron photons", Nuclear Instruments and Methods in Physics Research B, vol. 320, pp. 37–45, 2014.

[20] Y. Chauhan, A. Kumar, S. Puri, At. Data Nucl. Data Tables, vol. 95(4), pp. 475-500, 2009.

[21] S. Arsene, J. Bai, P. Bompard, "Hydride Embrittlement and Irradiation Effects on Hoop Mechanical Properties of Pressurised Wtaer Reactor and Boiling Water Reactor ZIRCALOY Cladding Tubes: Part I: Hydride Embrittlement in Stress-relieved, Annealed and Recrystallized ZIRCALOYs at 20^0C and 300^0C" Metallurgical and Materials Transactions A, vol. 34, pp. 553-566, 2003.

[22] G. Choudhuri, D. Srivastava, K. Gurumurthy, B. Shah, "Optimization of Stress Relief Heat Treatment of PHWR Pressure Tubes (Zr-25Nb alloy)" Journal of Nuclear Materials, vol. 383, pp. 178-182, 2008.

[23] M.K. Tiwari, and Gangadhar Das, "An interactive graphical user interface (GUI) for the CATGIXRF program for microstructural evaluation of thin film and impurity doped surfaces", X-Ray Spectrom., vol. 45, pp. 212–219, 2016.

[24] B. Shukla, N. R. S. Kumar, G. Kaur, N. V. C. Shekar, A. K. Sinha, "Compressibility and thermal expansion study of -UZr2 at high pressure and high temperature", J. Alloy. Comp. vol. 813, pp. 152214-18, 2020 *and references therein.*

[25] N. L. Misra, A. K. Yadav, S. Dhara, S. K. Mishra, R. Pathak, A. K. Poswal, S. N. Jha, A. K. Sinha, D. Bhattacharya, "Charcterisation of Sb doped Bi2UO6 solid solutions by x-ray diffraction and x-ray absorption spectroscopy", Anal. Sciences, vol. 29, pp. 579-584, 2013.